A least-squares shot-profile application of time-lapse inverse scattering theory

Mostafa Naghizadeh and Kris Innanen

ABSTRACT

The time-lapse imaging problem is addressed using least-squares shot-profile migration. The procedure for designing forward (de-migration) and adjoint (migration) operators of shot-profile wave-equation migration algorithm is explained. The least-squares optimization of the problem is achieved using conjugate gradients. Two main approaches for least-squares shot-profile migration of time-lapse data namely, inversion of difference data and joint inversion, are discussed. Some practical considerations for performance of least-squares shot-profile migration are investigated using synthetic data examples. Also, a synthetic data examples is provided for examining the time-lapse shot-profile migration of difference data.

INTRODUCTION

Time-lapse seismic surveys have become an industry standard in exploration seismology. It consists of an operation to acquire and process multiple seismic surveys, repeated at the same location over a period of time (Lumley, 2001). It can be utilized for various purposes such as reservoir monitoring, CO2 sequestration, and environmental studies. The main problem with processing time-lapse seismic surveys lays in the fact that multiple surveys can not be acquired with the exact same geometry. Therefore, efficient processing methods are necessary in order to account for the mismatch between the surveys.

Recently, least-squares migration and wave-field propagation techniques have also received special attention in the geophysical community. The corner stone for almost all of these methods is the Born approximation to the wave equation. Born approximation is an attempt to linearize the wave equation (Clayton and Stolt, 1981) and therefore obtaining a suitable set of linear equations to be solved using least-squares method. To solve a linear system of equation with huge number of model and data entries (As this is the case with migration of seismic data), it is suitable to create a set of forward and adjoint operators (Kaplan et al., 2010b). The forward operator maps the image (Model) to seismic data (de-migration) and conversely the adjoint operator maps the seismic data to the model.

In this paper, we review the derivation of forward and adjoint operators for shot-profile migration for a constant velocity medium. The derivation is closely follows the one explained in Kaplan et al. (2010a). Then, some practical considerations for optimal performance of least-squares shot-profile migration will be explained using synthetic data examples. Next, we will investigate possible least-square shot-profile migration approaches for handling time-lapse data set. Finally, a synthetic example for time-lapse shot-profile migration is provided.

THEORY

Shot-profile migration and de-migration operators

Least-squares migration offers a robust numerical appoach to deal with migration of incomplete seismic data sets (Nemeth et al., 1999). It depends on building de-migration and migration operators, which map from model-space to data-space (the forward operator), and from data-space to model-space (adjoint operator), respectively. For shot-profile migration the Born approximation is used, which is a first order approximation to the scattering potential. Here, we summarize the constant velocity shot-profile wave-equation migration and de-migration operators.

The forward operator (de-migration) models the scattered seismic wave-field using the Born approximation under the assumption of an acoustic and constant velocity Green's function so that (Kaplan et al., 2010a),

$$\psi_s(\mathbf{x}_g, z_g|\mathbf{x}_s, z_s; \omega) = f(\omega) \iint_{-\infty}^{\infty} G_0(\mathbf{x}_g, z_g|\mathbf{x}', z'; \omega) \left(\frac{\omega}{c_0}\right)^2 \alpha(\mathbf{x}', z') G_0(\mathbf{x}', z'|\mathbf{x}_s, z_s; \omega) d\mathbf{x}' dz', \tag{1}$$

where G_0 is a Green's function for constant acoustic wave-speed c_0, and such that,

$$G_0(\mathbf{x}_g, z_g|x', z'; \omega) = \frac{1}{2\pi} \int_{-\infty}^{\infty} \left(-\frac{1}{i4k_{gz}}\right) e^{-i\mathbf{k}_{gx}\cdot(\mathbf{x}'-\mathbf{x}_g)} e^{ik_{gz}|z_g-z'|} d\mathbf{k}_{gx}. \tag{2}$$

In equation 1, α is the first order approximation to the scattering potential. Within the context of least-squares migration and SPDR, α is the model (a migrated shot gather). The forward operator in equation 1 describes the mapping from the approximate scattering potential α (the model-space) to the scattered wave-field ψ_s (the data-space) recorded at geophone positions $(\mathbf{x}_g, z_g)$ where $\mathbf{x}_g = (x_g, y_g)$, and due to the seismic source $f(\omega)$ located at $(\mathbf{x}_s, z_s)$ where $\mathbf{x}_s = (x_s, y_s)$. Equation 1 integrates over all possible scattering points $(\mathbf{x}', z')$ where $\mathbf{x}' = (x', y')$. The vertical wave-number k_{gz} in equation 2 is given by the dispersion relation,

$$k_{gz} = sgn(\omega)\sqrt{\frac{\omega^2}{c_0^2} - \mathbf{k}_{gx}\cdot\mathbf{k}_{gx}}, \tag{3}$$

where $\mathbf{k}_{gx} = (k_{gx}, k_{gy})$ are the lateral wave-numbers (Fourier conjugate variables of $\mathbf{x}_g = (x_g, y_g)$). The dispersion relation plays a role in understanding the null-space of the de-migration operator.

After a series of mathematical derivations which its detail can be found in Kaplan et al. (2010a) we derive an efficient numerical forward and adjoint operators for shot profile migration. Let's assume that the earth model is partitioned into n_z layers of constant thickness Δz. First, we define $v_{s(l)}$ for $l = 1 \ldots n_z$ such that,

$$\begin{aligned} v_{s(1)}(\mathbf{k}_{gx}, \omega; \mathbf{x}_s) &= u_{p(1)}(\mathbf{k}_{gx}, \omega) g(\mathbf{k}_{gx}, \mathbf{x}_s, \omega) \\ v_{s(l)}(\mathbf{k}_{gx}, \omega; \mathbf{x}_s) &= \Delta u_p(\mathbf{k}_{gx}, \omega) v_{s(l-1)}(\mathbf{k}_{gx}, \omega; \mathbf{x}_s), \end{aligned} \tag{4}$$

where $u_{p(1)} = \exp(ik_{gz}(z_1 - z_0))/(i4k_{gz})$ and $\Delta u_p = \exp(ik_{gz}\Delta z)$ are phase shift operators and $g(\mathbf{k}_{gx}, \mathbf{x}_s, \omega) = 2\pi f(\omega) e^{-i\mathbf{k}_{gx}\cdot\mathbf{x}_s}$ is the synthetic source term. Second, we define $v_{r(l)}$

so that,

$$\begin{aligned} v_{r(1)}(\mathbf{k}_{gx},\omega) &= u_{p(1)}(\mathbf{k}_{gx},\omega) \\ v_{r(l)}(\mathbf{k}_{gx},\omega) &= \Delta u_p(\mathbf{k}_{gx},\omega) v_{r(l-1)}(\mathbf{k}_{gx},\omega). \end{aligned} \tag{5}$$

Then the forward operator becomes,

$$\psi_s(\mathbf{k}_{gx},\omega;\mathbf{x}_s) = \left(\frac{\omega}{c_0}\right)^2 \Delta z \sum_{l=1}^{n_z} v_{r(l)}(\mathbf{k}_{gx},\omega)\mathcal{F}\left[\mathcal{F}^* v_{s(l)}(\mathbf{k}_{gx},\omega;\mathbf{x}_s)\right]\alpha(\mathbf{x}_g,z_l;\mathbf{x}_s). \tag{6}$$

Equations 4-6 constitute an algorithm that implements the de-migration operator and the main load of computation is in the two two-dimensional Fourier transforms required per depth and frequency.

The implementation of the adjoint operator is also derived using two iterations. First, we define $v^*_{s(l)}$ for $l = 1 \ldots n_z$ so that,

$$\begin{aligned} v^*_{s(1)}(\mathbf{k}_{gx},\omega;\mathbf{x}_s) &= u^*_{p(1)}(\mathbf{k}_{gx},\omega) g^*(\mathbf{k}_{gx},\mathbf{x}_s,\omega) \\ v^*_{s(l)}(\mathbf{k}_{gx},\omega;\mathbf{x}_s) &= \Delta u^*_p(\mathbf{k}_{gx},\omega) v^*_{s(l-1)}(\mathbf{k}_{gx},\omega;\mathbf{x}_s). \end{aligned} \tag{7}$$

Second, we define $v^*_{r(l)}$ for $l = 1 \ldots n_z$ so that,

$$\begin{aligned} v^*_{r(1)}(\mathbf{k}_{gx},\omega;\mathbf{x}_s) &= u^*_{p(1)}(\mathbf{k}_{gx},\omega) \psi_s(\mathbf{k}_{gx},\omega;\mathbf{x}_s) \\ v^*_{r(l)}(\mathbf{k}_{gx},\omega;\mathbf{x}_s) &= \Delta u^*_p(\mathbf{k}_{gx},\omega) v^*_{r(l-1)}(\mathbf{k}_{gx},\omega;\mathbf{x}_s). \end{aligned} \tag{8}$$

Then, the adjoint operator becomes,

$$\alpha^\dagger(\mathbf{x}_g,z_l;\mathbf{x}_s) = \Delta\omega \sum_j \left(\frac{\omega_j}{c_0}\right)^2 \left[\mathcal{F}^* v^*_{s(l)}(\mathbf{k}_{gx},\omega;\mathbf{x}_s)\right] \mathcal{F}^* v^*_{r(l)}(\mathbf{k}_{gx},\omega;\mathbf{x}_s), \tag{9}$$

again requiring two two dimensional Fourier transforms per depth and frequency. Equation 9 is shot-profile migration for a constant velocity reference medium.

Least-squares shot-profile migration

The cost function for weighted least-squares inversion of shot-profile migration can be expressed as

$$\phi(\mathbf{m}) = ||\mathbf{W}_d(\mathbf{d}^{obs} - \mathbf{L}\mathbf{m})||_2^2 + \mu||\mathbf{W}_m\mathbf{m}||_2^2 \tag{10}$$

$$= \phi_d(\mathbf{m}) + \mu\phi_m(\mathbf{m}), \tag{11}$$

where $\mathbf{d}^{obs}$ is the observed data (shot record), $\mathbf{m}$ is the subsurface model and $\mathbf{L}$ is the forward (de-migration) operator. Also, $\mathbf{W}_d$ are data weights, and $\mathbf{W}_m$ are model weights. It is convenient to partition the cost function into two components ϕ_d and ϕ_m, with ϕ_d being the data misfit function, and ϕ_m being the model-norm function. The parameter μ allows for a trade-off between fitting the observed data, and honoring the model-norm. Finding the minimum of equation 13 results in the normal equations,

$$(\mathbf{L}^H\mathbf{W}_d^H\mathbf{W}_d\mathbf{L} + \mu\mathbf{W}_m^H\mathbf{W}_m)\mathbf{m} = \mathbf{L}^H\mathbf{W}_d^H\mathbf{W}_d\mathbf{d}^{obs}, \tag{12}$$

which is solved to find an optimal scattering potential.

Least-squares shot-profile migration for time-lapse application

Inversion of difference section

The first approach to apply least-squares shot-profile migration for time-lapse surveys is to use the difference data between base and monitor surveys. Innanen and Naghizadeh (2010) show that such an approximation is valid in the linear approximation of inverse scattering theory. The linear system of equations can be expressed as

$$\phi(\mathbf{m}_{diff}) \quad = \quad ||\mathbf{W}_d(\mathbf{d}_{diff} - \mathbf{L}\mathbf{m}_{diff})||_2^2 + \mu||\mathbf{W}_m\mathbf{m}_{diff}||_2^2, \tag{13}$$

where $\mathbf{m}_{diff}$ and $\mathbf{d}_{diff}$ are the difference model and data difference sections, respectively. For difference data one can use exactly the same adjoint and forward operators from ordinary least-squares shot-profile migration. In the examples section we will provide a simple example for this type of time-lapse inversion.

Joint inversion of base and monitor surveys

Another alternative for time-lapse inversion is the joint inversion. Some modifications are required for applying joint least-squares shot-profile migration for time-lapse data. Let's $\mathbf{d}_b$ and $\mathbf{d}_m$ represent the data sets for base and monitor surveys, respectively. Similarly, $\mathbf{m}_b$ and $\mathbf{m}_m$ represent the subsurface scattering potential at base and monitor survey, respectively. One can make an augmented linear system of equation for time-lapse survey

$$\begin{bmatrix} \mathbf{d}_b \\ \mathbf{d}_m \end{bmatrix} = \begin{bmatrix} \mathbf{L}_b & 0 \\ 0 & \mathbf{L}_m \end{bmatrix} \begin{bmatrix} \mathbf{m}_b \\ \mathbf{m}_m \end{bmatrix} + \begin{bmatrix} \mathbf{n}_b \\ \mathbf{n}_m \end{bmatrix}, \tag{14}$$

where $\mathbf{n}_b$ and $\mathbf{n}_m$ are noises in base and monitor surveys, respectively. A regularized solution can be found by minimizing the following cost function (Ayeni and Biondi, 2010)

$$\begin{aligned} J = & \left\| \begin{bmatrix} \mathbf{L}_b & 0 \\ 0 & \mathbf{L}_m \end{bmatrix} \begin{bmatrix} \mathbf{m}_b \\ \mathbf{m}_m \end{bmatrix} - \begin{bmatrix} \mathbf{d}_b \\ \mathbf{d}_m \end{bmatrix} \right\|^2 \\ & + \left\| \begin{bmatrix} \mu_b\mathbf{R}_b & 0 \\ 0 & \mu_m\mathbf{R}_m \end{bmatrix} \begin{bmatrix} \mathbf{m}_b \\ \mathbf{m}_m \end{bmatrix} \right\|^2 \\ & + \left\| \begin{bmatrix} \lambda_b\mathbf{D}_b & \lambda_m\mathbf{D}_m \end{bmatrix} \begin{bmatrix} \mathbf{m}_b \\ \mathbf{m}_m \end{bmatrix} \right\|^2, \end{aligned} \tag{15}$$

Where $\mathbf{R}_b$ and $\mathbf{R}_m$ are model regularization terms and $\mathbf{D}_b$ and $\mathbf{D}_m$ are temporal regularization terms. Model regularization terms impose specific restrictions on each of the base and monitor surveys while the temporal regularization highlights some relationship between the base and monitor surveys. The model regularization can be in the form of smoothness or sparseness for spatial dimensions and the temporal regularization can be a derivative operator serving to magnify the differences between the models.

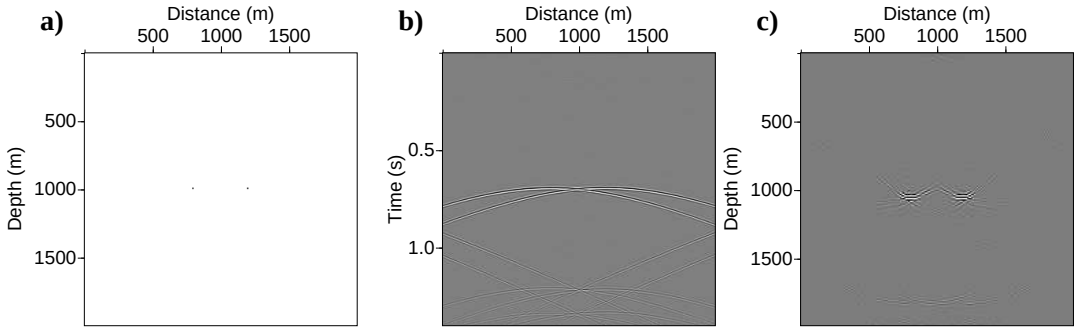

FIG. 1. Modeling and migration of two scatterers without zero-padding of the spatial axis. a) Scattering model. b) Forward modeled data. c) Adjoint model.

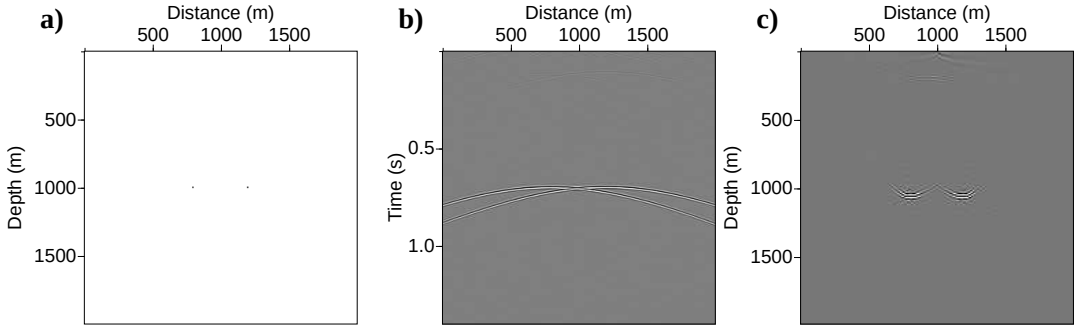

FIG. 2. Modeling and migration of two scatterers with zero-padding of the spatial axis. a) Scattering Model. b) Forward modeled data. c) Adjoint model.

EXAMPLES

Implementation of shot-profile migration

Several practical issues need to be taken into account for an efficient implementation of the least-squares shot-profile migration. Since the theoretical application of wave-equation migration method is developed in the Fourier domain, one has to be aware of the possible artifacts that can be produced in the Fourier domain. One of the important issues is the proper zero-padding of both data and model spaces to avoid the wrap-around artifact in the Fourier domain. Figure 1 shows a simple example of the outputs of forward and adjoint operators of shot-profile migration without zero-padding. Figure 1a shows the original model with two point scatterers at $(x, z) = \{(750, 1000), (1250, 1000)\}$. The source is located at $(x_s, z_s) = (1000, 0)$. Figure 1b shows the output of forward modeling operator (de-migration). There are high amplitude artifacts at the bottom of the shot gather. Figure 1c shows the output of applying adjoint operator (migration) on the synthetic data in Figure 1b. The adjoint model also suffers from some artifact due to no zero-padding of the model and data spaces. Figure 2 shows the same modeling test as in Figure 1 but this time with proper zero-padding of the model and data spaces. Both the data (Figure 2b) and the adjoint model (Figure 2c) spaces are now artifact-free.

Figure 3 shows another test with point scatterers located as the same location as the

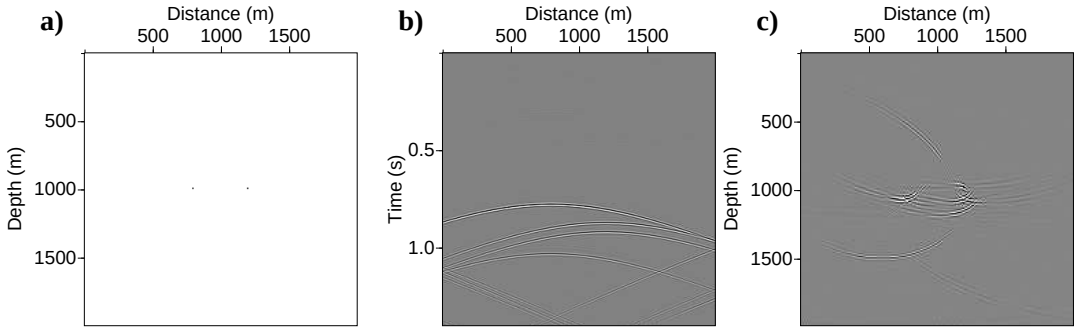

FIG. 3. Modeling and migration of two scatterers without zero-padding of the spatial axis. a) Scattering Model. b) Forward modeled data. c) Adjoint model.

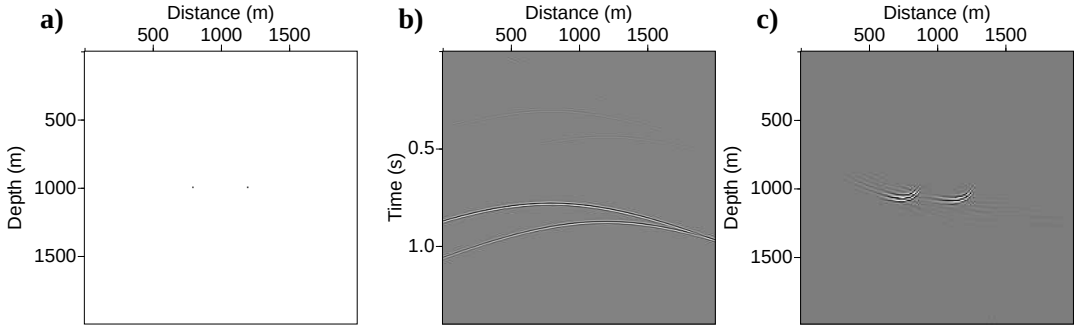

FIG. 4. Modeling and migration of two scatterers with zero-padding of the spatial axis.a) Scattering Model. b) Forward modeled data. c) Adjoint model.

model in Figure 1a. For this test the source is located at $(x_s, z_s) = (0, 0)$. Figures 3b and 3c show the outputs for data and adjoint model spaces with no zero-padding, respectively. Figures 4b and 4c show the data and model spaces after using proper zero-padding for both model and data spaces. It is clear that zero-padding has eliminated great amount of artifacts in both data and model spaces. Also notice that the quality of imaging for point scatterers is directly related to the aperture cover of the source.

In the next example (Figure 5a), we placed the point scatterers in different depths $(x, z) = \{(750, 750), (1250, 1250)\}$. Figures 5b and 5c show the data and adjoint model spaces of shot-profile migration without zero-padding. The artifacts due to this careless handling of the model and data spaces can be seen in both spaces. Figures 6b and 6c show the data and adjoint model spaces of shot-profile migration with zero-padding. The artifacts due to the sharp edge of model and space are now less apparent.

Figure 7a shows a synthetic model of a geological fault-like structure. Figures 7b and 7c show the data and adjoint model spaces using the forward and adjoint operators, respectively. The source in this example is located at $(x_s, z_s) = (500, 0)$. It is clear that the migration has a cone of aperture on which the imaging is carried out with high resolution. As the location of the scatterers get further from the shot, the resolution of final adjoint model deteriorates. This example has been carried out using only a single shot but one can have several shots (as it is the case with seismic surveys) and the contribution from various

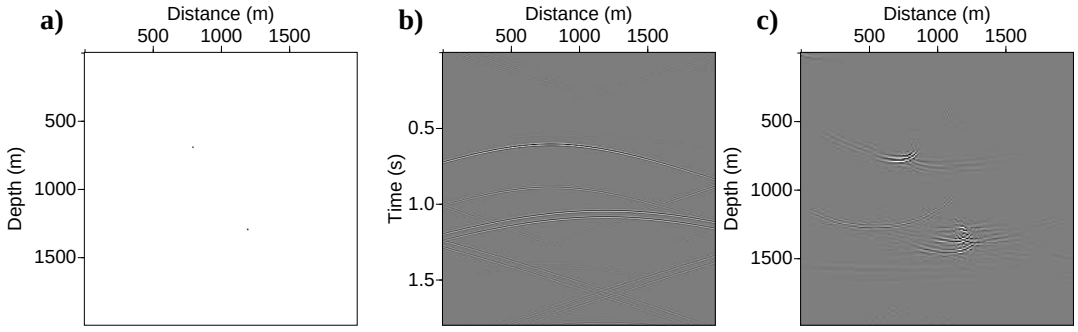

FIG. 5. Modeling and migration of two scatterers without zero-padding of the spatial axis. a) Scattering Model. b) Forward model-led data. c) Adjoint model.

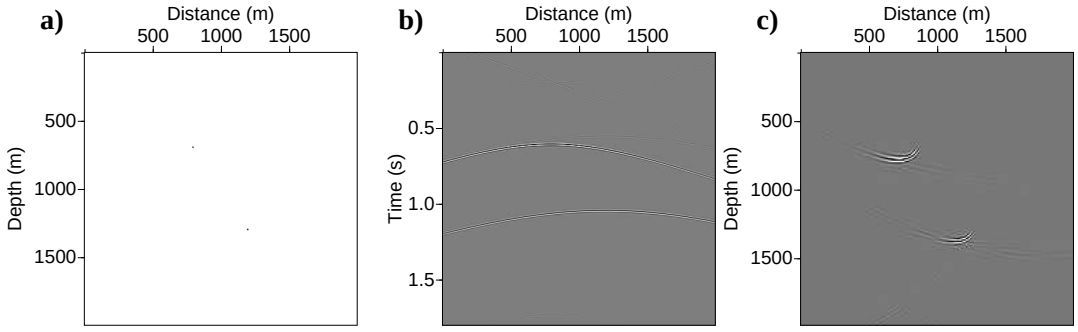

FIG. 6. Modeling and migration of two scatterers with zero-padding of the spatial axis. a) Scattering Model. b) Forward modeled data. c) Adjoint model.

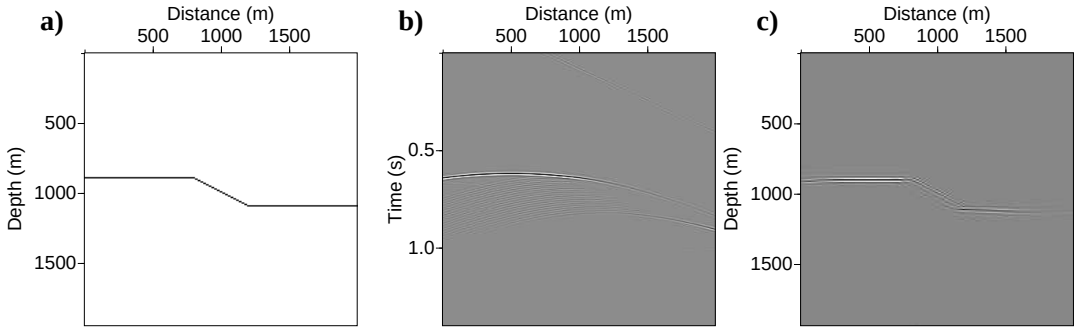

FIG. 7. Modeling and migration of a fault-like structure. a) Scattering Model. b) Forward modeled data. c) Adjoint model.

shots can be summed up to make final adjoint model.

Time-lapse migration of difference data

Here, we provide a simple least-squares shot-profile migration example for difference data of a synthetic time-lapse survey. Figures 8a and 8b show the velocity models used for the base and monitor surveys, respectively. The model consists of two layers with velocities 1500 and 2500 m/s for the top and bottom layers, respectively. In the base survey the boundary is located at the depth equal to 200 m while in the monitor survey it has been relocated to the depth of 300 m. We applied the forward modeling using finite difference method to create the data associated with the base (Figure 9a) and monitor (Figure 9b) surveys. The sources is located at $(x_s, z, s) = (0, 50)$ for both base and monitor surveys. Also, the receivers are located at the depth equal to 50 m. Figure 9c shows the wavelet used for producing the synthetic data.

Figure 10a shows the difference between the modeled data for base and monitor surveys. Figure 10b shows the result of least-square shot-profile migration applied on the difference data. The derived adjoint model has the reflecting boundaries at right depth. However, the resolution is reduced at horizontal locations fur from the horizontal location of the source. Utilizing more shots acquired on the surface can resolve the reflectors with high accuracy in the adjoint model.

DISCUSSION AND FUTURE WORKS

It is a main concern that the computational costs of time-lapse survey migration can be very expensive. In fact, the process of joint migration of time-lapse surveys will require individual migration and de-migration of each surveys plus intermittent steps needed for spatial and temporal regularizations. Therefore, it is desirable to design a fast and efficient imaging technique that only focus on specific targets of interest. A new signal processing tool called cross-wavelet transform (Grinsted et al., 2004) which is used to highlight the similarities as well as the differences between two specific data sets can be considered as a proper candidate for this task. This transform can also be replaced by the Fast Generalized Fourier Transform (FGFT) (Naghizadeh and Innanen, 2010) in order to account for spatial

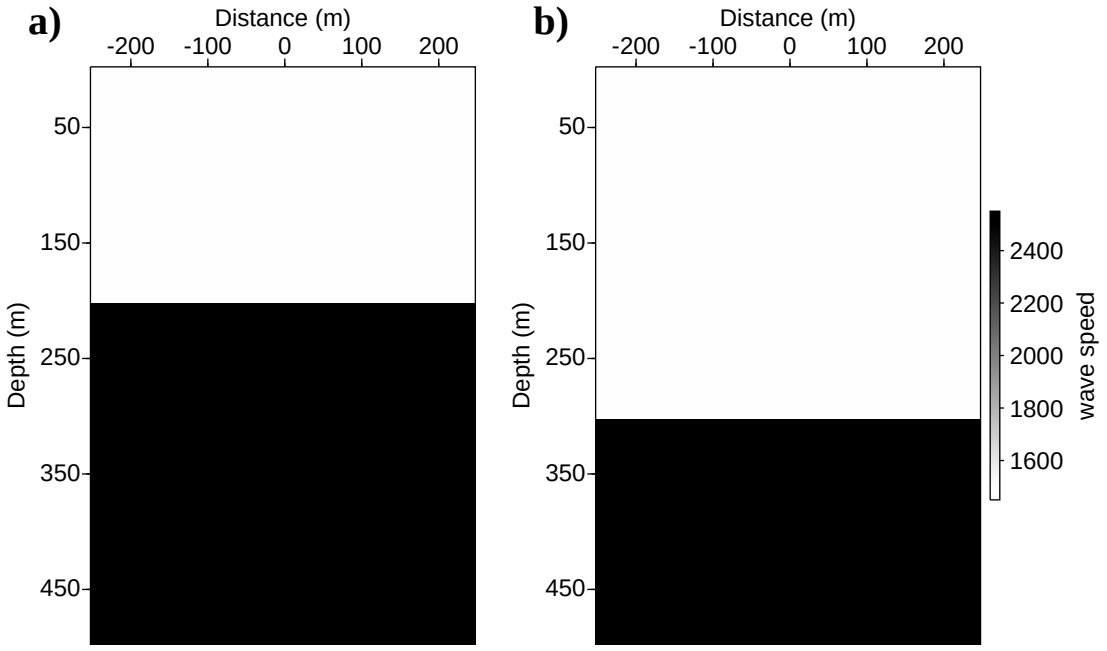

FIG. 8. a) Velocity model for base survey. b) Velocity model for monitor survey.

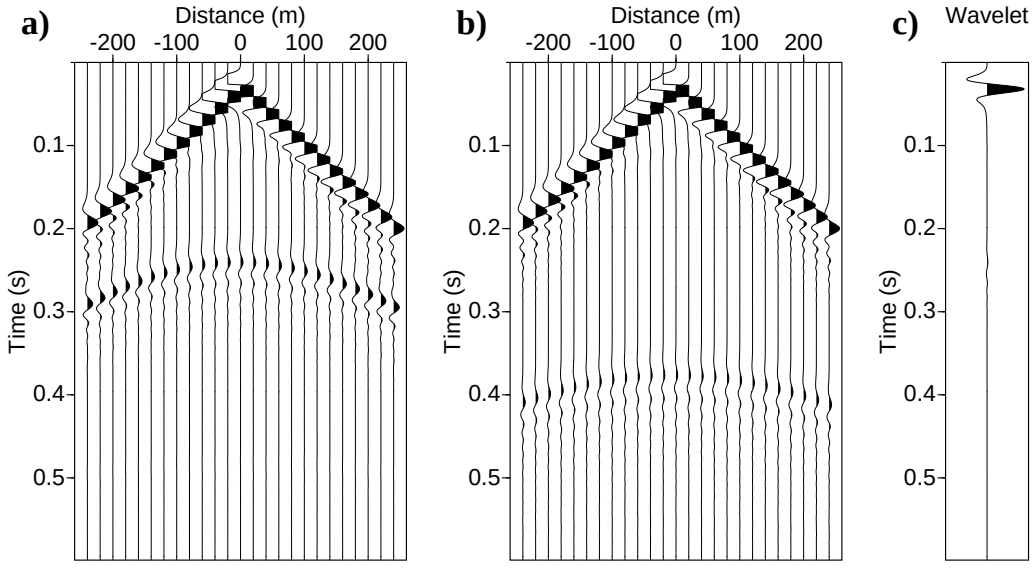

FIG. 9. Finite difference modeled data for the base (a) and monitor (b) surveys. c) Wavelet used for making the synthetic data.

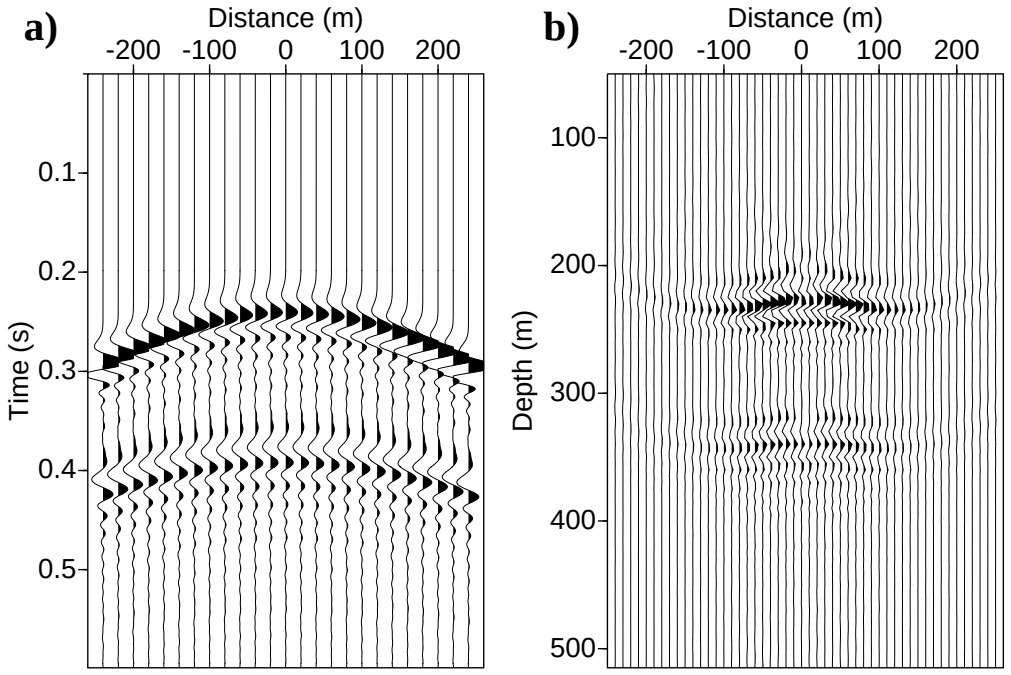

FIG. 10. a) The difference section between the base and monitor surveys. b) Migrated data using the least-squares shot-profile migration.

and temporal non-stationarity of the time-lapse seismic data.

The geometry of various time-lapse surveys often differs for base and monitor surveys. This can turn into a big problem since the main purpose of time-lapse surveys is to detect the differences only caused by the changes in the parameters of subsurface rather than acquisition mismatches. Therefore, it might be necessary to use robust interpolation methods to synthesize one of the surveys with the same geometry of another survey. There are several robust and efficient seismic data interpolation methods which can be used for this purpose (Naghizadeh and Sacchi, 2007, 2009, 2010).

CONCLUSIONS

Least-squares shot-profile migration is used for imaging the difference data between the base and monitor surveys in time-lapse studies. The algorithm contains forward (demigration) and adjoint (migration) operators which allows the usage of conjugate gradient method. The proposed method can be used for both data differences as well as joint inversion of multiple surveys. Proper spatial and temporal regularization terms such as smoothness or sparseness constraints can be incorporated into the algorithm to obtain a robust solution. The algorithm has a high computational costs which can be mitigated by designing a fast and efficient imaging tool. One can utilize new transform domains such as FGFT to ease the plane-wave assumption of migration tools to obtain a fast migration algorithm.

ACKNOWLEDGEMENTS

We thank the financial support of the sponsors of the Consortium for Research in Elastic Wave Exploration Seismology (CREWES) at the University of Calgary. We also thank Dr. Sam T. Kaplan for his helpful discussions and comments.

REFERENCES

Ayeni, G., and Biondi, B., 2010, Target-oriented joint least-squares migration/inversion of time-lapse seismic data sets: Geophysics, **75**, No. 3, R61–R73.

Clayton, R. W., and Stolt, R. H., 1981, A born-wkbj inversion method for acoustic reflection data: Geophysics, **46**, No. 3, 1559–1567.

Grinsted, A., Moore, J. C., and Jevrejeva, S., 2004, Application of the cross wavelet transform and wavelet coherence to geophysical time series: Nonlinear Processes in Geophysics, **11**, 561–566.

Innanen, K. A., and Naghizadeh, M., 2010, Direct determination of time-lapse perturbations from seismic reflection data: CREWES Annual report.

Kaplan, S. T., Naghizadeh, M., and Sacchi, M. D., 2010a, Data reconstruction with shot-profile least-squares migration: Geophysics, **75**, No. 6.

Kaplan, S. T., Routh, P. S., and Sacchi, M. D., 2010b, Derivation of forward and adjoint operators for least-squaresshot-profile split-step migration: Geophysics, **75**.

Lumley, D. E., 2001, Time-lapse seismic reservoir monitoring: Geophysics, **66**, No. 1, 50–53.

Naghizadeh, M., and Innanen, K. A., 2010, Seismic data interpolation using a fast generalized fourier transform: CREWES Annual report.

Naghizadeh, M., and Sacchi, M. D., 2007, Multistep autoregressive reconstruction of seismic records: Geophysics, **72**, No. 6, V111–V118.

Naghizadeh, M., and Sacchi, M. D., 2009, *f-x* adaptive seismic-trace interpolation: Geophysics, **74**, No. 1, V9–V16.

Naghizadeh, M., and Sacchi, M. D., 2010, Beyond alias hierarchical scale curvelet interpolation of regularly and irregularly sampled seismic data: Geophysics, **75**, No. 6.

Nemeth, T., Wu, C., and Schuster, G. T., 1999, Least-squares migration of incomplete reflection data: Geophysics, **64**, 208–221.